PERTURBATION OF VORTEX INDUCED VIBRATIONS ON A SQUARE SECTION CYLINDER

Pascal Hémon

Hydrodynamics Laboratory (LadHyX) Ecole Polytechnique – CNRS, Palaiseau, France

Françoise Santi

Department of Mathematics, CNAM, Paris, France

ABSTRACT

This paper addresses the vibration of a square section cylinder due to the alternate vortex shedding at moderate Reynolds number (3500). The numerical investigation is focused on the perturbation of the vortex shedding in order to decrease the amplitude of the vibrations at lock-in. By analyzing the unsteady flow results, we show that a control technique spatially localized at the surface of the cylinder, can be efficient only if the mean flow is modified, or/and that the energy input, i.e. the cost function, becomes very large.

1. INTRODUCTION

Vibrations induced by alternate vortex shedding and their control have been widely studied with circular cylinders. In this paper, we deal with such kind of vibrations on a square section cylinder at moderate Reynolds number (3500). The numerical investigation is focused on the perturbation of the vortex shedding in order to decrease the amplitude of the vibration at lock-in.

The essential feature of a square cylinder configuration is the fixed point of flow separation at the leading-edge corners which leads to unstable shear layers on both lateral faces of the section. At moderate Reynolds number, the Kármán vortex street which develops in the far wake leads to the unsteady lift. When its frequency is close to that of a structural mode high amplitude vibrations can occur by lock-in.

There exists a large number of techniques for perturbing or controlling these vibrations: Kubo et al. (1996) used small rotating cylinders flush mounted at the corners of the square cylinder. Small vibrating leading edge flaps have been tested by Li et al. (2003). More recently, Cheng et al. (2003) proposed to implement oscillations of a lateral boundary, as presented in Figure 1. The actuation consists in forcing a small amplitude oscillation *A(t)* of one of the lateral boundaries of the cylinder by means of a piezo-electric actuator. This control scheme is of the opened-loop type and

seems efficient when the actuator frequency is out of the lock-in range. Otherwise there is enhancement of the vibrations.

The purpose of this paper is to show that such a control or perturbation technique is expensive in energy due to the robustness of the vortex shedding process. First we validate our numerical tool by comparison with literature data. The differences between the oscillating non perturbed case and the perturbed case are then studied, notably with the help of biorthogonal decompositions of the local lift distribution.
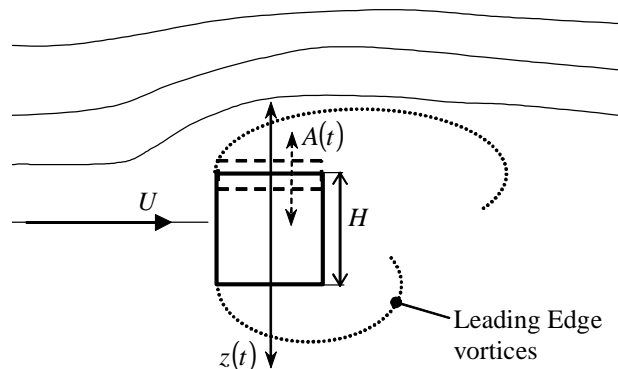

Figure 1 : Sketch of the studied configuration.

2. NUMERICAL TECHNIQUE

The physical model is formulated with the full incompressible 2D Navier-Stokes equations without turbulence modelling. The solver is based on a Lagrangian-Galerkin method. A mixed variational formulation of the full equations is implemented with a finite element approximation for space discretization. The convective problem is treated using a characteristic method, while the Stokes step is processed by an implicit algorithm. Low order characteristic methods are known to be diffusive on a large mesh but the region of interest (around the cylinder) is discretized, so that a first order derivative approximation with a fractional step characteristic method can be used.

For the cylinder motion, the numerical simulations consider forced oscillations $y(t)$ normal to the flow as in Figure 1. Since the movement is that of a rigid body, the vibrations of the structure are simulated by applying the movement on the external boundary conditions. The computations are then performed in the reference frame of the body, and the grid acceleration term is taken into account in the equations.

The effect of the actuator acting as a perturbation of small amplitude is simulated with an unsteady boundary condition. The normal velocity $\dot{A}(t)$ is then prescribed at the upper surface of the cylinder (see Figure 1).

3. STATIC CASE

In a first step, the static case, without motion and without perturbation is simulated in order to validate the numerical technique. The Reynolds number based on the side H of the cylinder is 3500.

The computed aerodynamic coefficients of the cylinder are presented in Table 1. The mean drag, its root-mean-square (RMS), the RMS value of the lift, the Strouhal number and the base pressure coefficient are globally in agreement with literature data (Bearman & Obasaju, 1982 ; Davis & Moore 1982 ; Norberg, 1993 ; Verstappen, 2002 ; Yi & Okajima 1996). The RMS amplitude of the lift is more or less twice that observed on a circular cylinder (Bearman & Obasaju, 1982), due to the large lateral walls of the square shape which are submitted to the stalled flow.
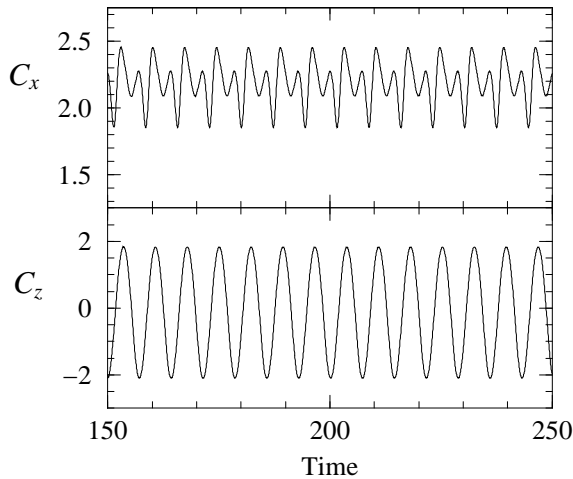

Figure 2 : Time history of drag and lift forces, static case

A sample of drag and lift coefficients versus dimensionless time is given Figure 2, after a stationary state has been reached. We can observe the standard oscillating behaviour, with the drag fluctuation at a frequency twice that of the lift force, which defines the Strouhal number of the alternate vortex shedding. The drag evolution, showing a subharmonic is typical of the moderate Reynolds number range (Davis & Moore, 1982).

4. OSCILLATING CASES

4.1 Non perturbed case

The cylinder is now put into motion at the frequency $St = 0.139$ of the vortex shedding in order to simulate the oscillating corresponding case, as in the experiments presented by Cheng et al. (2003). The imposed motion is sinusoidal:

$$z(t) = z_0 \sin(2\pi St\, t + \varphi). \qquad (1)$$

The motion amplitude z_0 is set to 8% of the dimension H of the section. Note that the results presented hereafter are for a stationary state in which the transient period between static case and oscillating one has been removed. Hence, the phase angle φ in equation (1) is not significant.

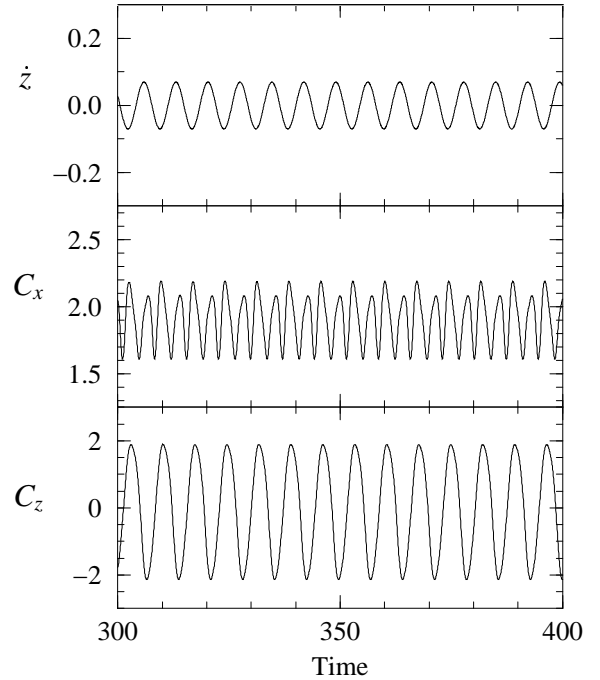Time histories of the force coefficients are given in Figure 3, together with the cylinder section velocity $\dot{z}$.

Figure 3 : Time history of drag and lift force, non perturbed oscillating case.

The resulting lift force is delayed of 30° with the cylinder displacement, which is in the range of the drastic change observed in the experimental results of Bearman and Obasaju (1982). Moreover, they noticed that the unsteady lift is increased by the

cylinder motion, which is found also by the present computation, as presented in Table 2. The mean drag decrease has also been found by Yi and Okajima (1996).

C_x mean	2.19
C_x RMS	0.16
C_z RMS	1.40
St	0.139
Cp base	-1.51

Table 1 : Computed aerodynamic coefficients of the static case

	(a)	(b)
C_x mean	1.92	2.14
C_x RMS	0.20	0.24
C_z RMS	1.44	1.46

Table 2 : Computed aerodynamic coefficients (a) non perturbed oscillating case ; (b) perturbed

4.2 Perturbed oscillating case

In this section, we now simulate the perturbed oscillating case using the parameters values presented by Cheng et al. (2003) in their experiments. The cylinder displacement remains similar to equation (1) with an amplitude z_0 decreased to 2% of H.

The displacement generated by the actuator is

$$A(t) = A_0 \sin(2\pi St_c\ t + \varphi), \qquad (2)$$

in which the control Strouhal number St_c is 0.1 and the amplitude A_0 is 2.8% of H. Once again, the phase angle is not significant at stationary state. Note also that the cylinder displacement is forced at another frequency. This will generate a very low frequency component (i.e. St-St_c) corresponding to the interaction between cylinder displacement and the actuator.

The resulting force coefficients are given in Table 2. The mean drag recovers more or less the value of the static cylinder, due to the vortex location closer to the base of the cylinder, thus decreasing the base pressure coefficient.

But the drag and lift, in terms of RMS value are not decreased as it is expected with the perturbation scheme and a deeper analysis of the results is necessary. Time histories are presented in Figure 4 with the cylinder velocity $\dot{z}$ and the perturbation velocity $\dot{A}$ (dotted line). It is interesting to notice that with the parameters chosen by Cheng et al. (2003), the velocity amplitude of the cylinder motion and that of the perturbation are of same order.

It is clear in Figure 4 that the drag is really perturbed, showing disorganized oscillations. Thus the RMS value is not a pertinent indicator because the corresponding spectrum shows a number of frequencies in the signal. However, this is not the case for the unsteady lift which shows indeed a quasi-sinusoidal evolution, weakly modulated at low frequency. The corresponding RMS value weakly perturbed is therefore pertinent.
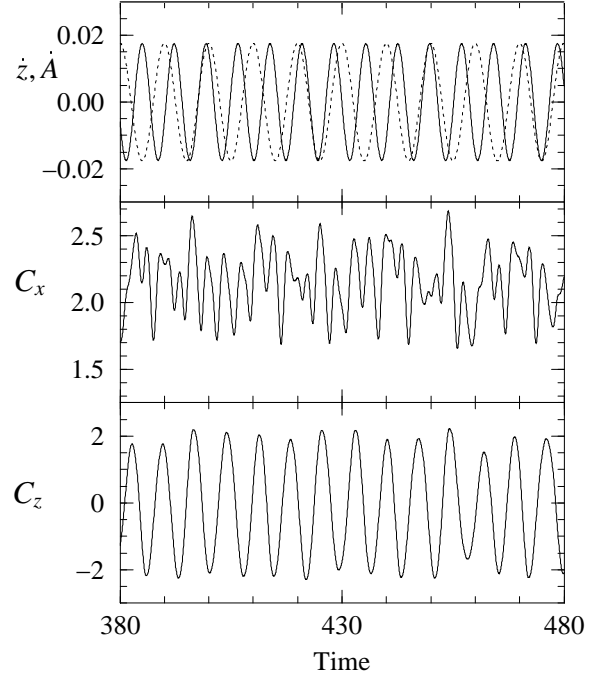

Figure 4 : Time history of drag and lift forces, perturbed oscillating case.

It must also be mentioned that, in another case not presented here due to limited length, we have simulated the enhancement of vortex shedding and of the lift by setting the perturbation frequency as the same value as the natural shedding (i.e. $St=St_c$). Results were in agreement with the similar experimental tests of Cheng et al. (2003).

5. COMPARISON AND ANALYSIS

5.1 Flow morphology

From the previous results, it seems that the perturbation scheme is not efficient enough to decrease the vortex shedding effect on the lift.

In Figure 5 the vorticity distribution, superimposed with contour of iso-pressure, are plotted at the instant of maximum lift, for the non perturbed (5a) and perturbed (5b) cases. We observe that the actuator injects locally an additional circulation which remains confined in the shear layer, as it can be seen on the upper

surface of the cylinder section (Figure 5 b). But the main wake vortices are not really influenced by the perturbation, which explain the results concerning the lift force.

Thus to overcome natural vortex shedding, the amplitude of the perturbation must be much larger than the one used here. This point will be discussed later.
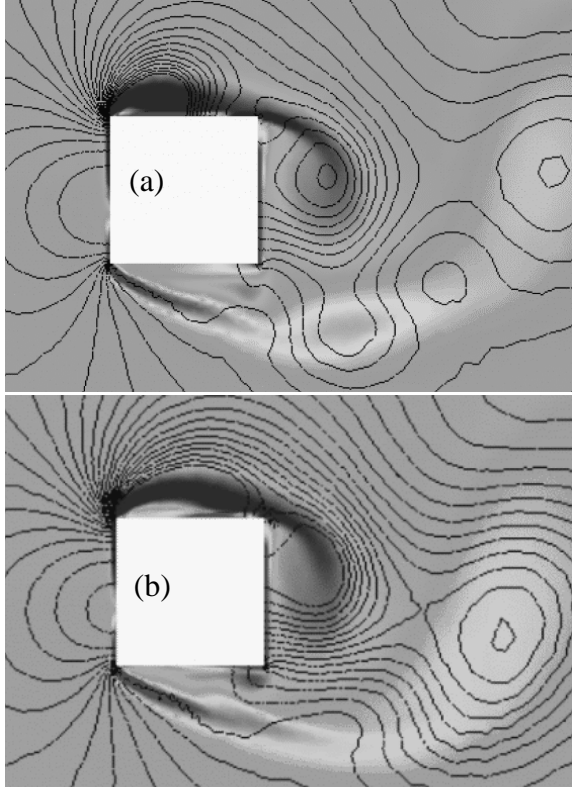

Figure 5 : Comparison of vorticity distributions, (a) non perturbed oscillating case; (b) perturbed

We perform now a deeper comparison of the two cases via the spatio-temporal analysis of the wall pressure coefficients. We use then the biorthogonal decomposition of the local lift force in the way that we have proposed recently (2003). This technique is useful in analysing complex signals by decomposing them into space functions (called topos) and time functions (called chronos) which are orthogonal between them and classified by order of importance.

For the oscillating case, the first 6 topos are shown Figure 6, with the wind blowing from left to right. The topos 1 is representative of the average value and is not relevant in the discussion. The corresponding chronos (with the first one removed) are presented Figure 7.

It is found that the main component of the lift (more than 99%) is given by the second chronos and topos. On the latter, it is interesting to note that

the downstream part of the two side boundaries have a low contribution in the global lift.
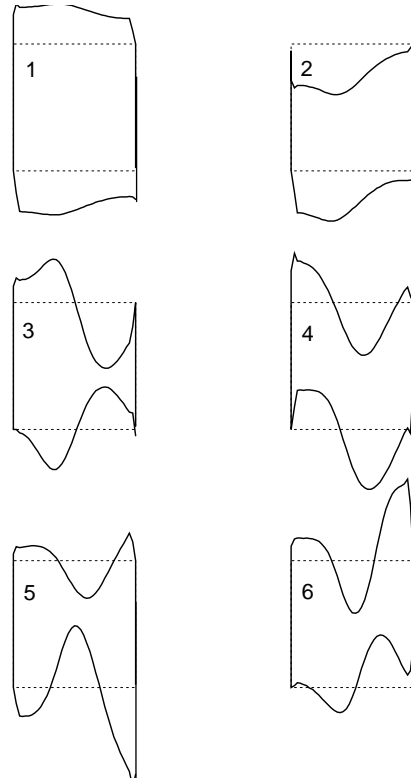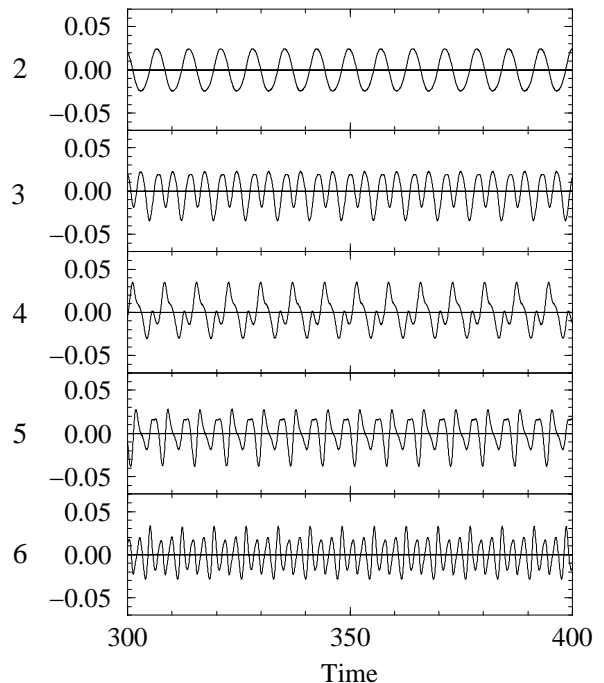

Figure 6 : Topos, oscillating case

Figure 7 : Chronos, oscillating case

For the perturbed oscillating case, the topos and the chronos are presented similarly in Figure 8 and 9. As for the non perturbed case, the second spatio-

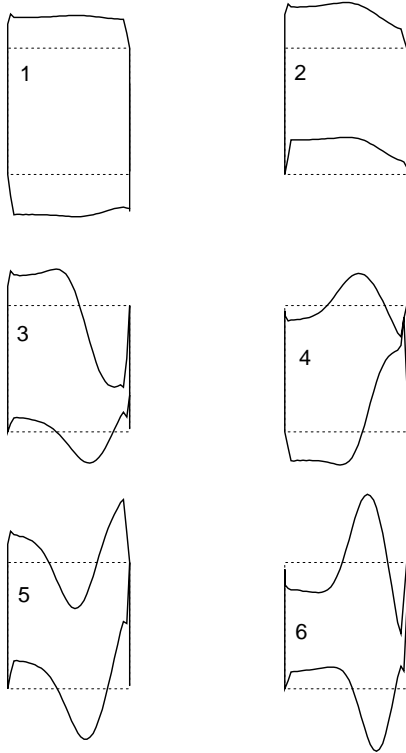temporal structure (topos + chronos) is sufficient to recompose the total lift at a level larger than 99%.

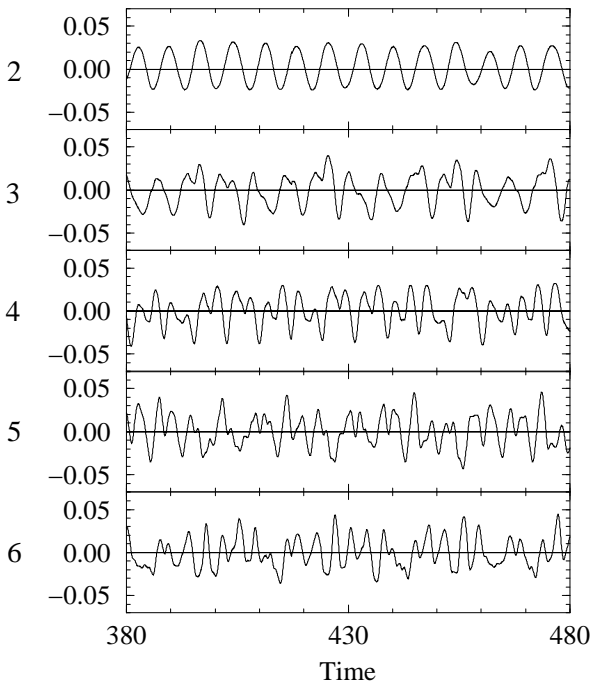*Figure 8 : Topos, perturbed oscillating case*

Figure 9 : Chronos, perturbed oscillating case

It is seen that the effects of the perturbation are located on the topos 3 and 4 because these structures do not appear in the decomposition of the non perturbed case. The topos 5 and 6 of the perturbed case indeed remain similar to the topos 4 and 5, respectively (eventually up to an arbitrary sign), of the non perturbed case.

Therefore the perturbation is shown to deeply modify the topos 3 of the non perturbed case, transforming this structure into the topos 3 and 4. Note that the non perturbed topos 3 has a symmetrical shape on the upper boundary compared to the lower boundary, leading to a zero lift force. For the perturbed case, this symmetry remains but it is decomposed into two topos (3 and 4). But these structures have a contribution in terms of global force which is representative of the drag (and the pitching moment) as it can be seen on the corresponding chronos that are similar to the drag time history.

The spatio-temporal analysis confirms then that the lift produced by the alternate vortex shedding is globally not perturbed by the actuator. The perturbation, localized inside the shear layer, is not able to disorganize the instability which is caused by the mean flow characteristics around the cylinder section.

5.2 Actuation

In fact this control scheme is very different of those of Kubo et al. (1996) or Li et al. (2003) for which the actuators are mounted at the leading edge corners of the square section. These corners are the separation points where the two shear layers are generated, thus where a perturbation will have a maximum efficiency.

The mean flow characteristics can be modified by these schemes, which can lead for instance to the generation of a steady lift, indicating a global change in the stall regions on the lateral faces of the section.

It is therefore interesting in the present case to consider the effects of the amplitude A_0 of the perturbation. Without oscillation of the cylinder, the main results are given in Table 3.

A_0	0	2.8 %	10 %
C_x mean	2.19	2.19	2.03
C_x RMS	0.15	0.21	0.22
C_z RMS	1.40	1.38	1.18

Table 3 : Computed aerodynamic coefficients without oscillation versus perturbation amplitude

It is seen that the small amplitude of 2.8 % is not able to modify significantly the unsteady lift value, and the mean drag remains unchanged.

To observe a decrease of the unsteady lift, the actuator amplitude has to be increased up to 10 %. In this case, the perturbation leads to a mean drag decrease of about 10 %, which means that the wake

morphology has also been modified. But the energy associated to the actuator, roughly proportional to the square of the perturbation amplitude, becomes then of the same order as that of the oscillations.

6. CONCLUSION

A numerical study of perturbed oscillations of a square section cylinder, due to alternate vortex shedding, has been presented. With the help of biorthogonal decomposition of the unsteady lift distribution, a spatio-temporal analysis was performed. We have shown that the perturbation scheme, similar to the experiments of Cheng et al. (2003), is efficient in perturbing the base flow only when the actuator amplitude is high.

Further work is to use another approach in understanding the sensitivity of the flow to perturbation. The idea is to use the results of the stability theory, based on the wake velocity profile as the base flow.

7. REFERENCES

BEARMAN, P.W. & OBASAJU, E.D., 1982 An experimental study of pressure fluctuations on fixed and oscillating square-section cylinders. *Journal of Fluid Mechanics* **119**: 297-321.

CHENG, L., ZHOU, Y. & ZHANG, M.M., 2003 Perturbed interaction between vortex shedding and induced vibration. *Journal of Fluids and Structures* **17**: 887-901.

DAVIS, R.W. & MOORE, E.F., 1982 A numerical study of vortex shedding from rectangles. *Journal of Fluid Mechanics*, **116**: 475-506.

HEMON, P. & SANTI, F., 2003 Applications of biorthogonal decompositions in fluid-structure interactions. *Journal of Fluids and Structures* **17**: 1123-1143.

KUBO, Y., MODI, V.J., KOTSUBO, C., HAYASHIDA, K. & KATO, K., 1996. Suppression of wind-induced vibrations of tall structures through moving surface boundary-layer control. *Journal of Wind Engineering and Industrial Aerodynamics* **61**: 181-194.

LI, Y.F., FLAY, R.G.J. & RICHARDS, P.J., 2003 Cross-wind excitation of a 2D square prism with vibrating leading edge flaps. *Journal of Wind Engineering and Industrial Aerodynamics* **91**: 185-197.

LUO, S.C., YAZDANI, Md.G., CHEW, Y.T. & LEE T.S., 1994 Effects of incidence and afterbody shape on flow past bluff cylinders. *Journal of Wind Engineering and Industrial Aerodynamics* **53**: 375-399.

NORBERG, C. 1993. Flow around rectangular cylinders: pressure forces and wake frequencies. *Journal of Wind Engineering and Industrial Aerodynamics* **49**: 187-196.

VERSTAPPEN R. 2002. On computing a turbulent square cylinder wake. *Conference on Bluff Body Wakes and Vortex-Induced Vibrations (BBVIV3)*, Port Douglas, Australia, 17-20 December.

YI D. & OKAJIMA A. 1996 Aerodynamic forces acting on an oscillating rectangular cylinder and the aeroelastic instabilities at moderate Reynolds number (experiments). *JSME International Journal*, series B, **39**(2): 343-353.